HAL
open science

Temperature-dependent rate constant for the reaction of F atoms with HNO 3

Yuri Bedjanian

To cite this version:

Yuri Bedjanian. Temperature-dependent rate constant for the reaction of F atoms with HNO 3. International Journal of Chemical Kinetics, 2019, 51 (10), pp.753-759. 10.1002/kin.21306 . hal-02268337

HAL Id: hal-02268337

https://hal.science/hal-02268337v1

Submitted on 12 Jan 2022

HAL is a multi-disciplinary open access archive for the deposit and dissemination of scientific research documents, whether they are published or not. The documents may come from teaching and research institutions in France or abroad, or from public or private research centers.

L'archive ouverte pluridisciplinaire **HAL**, est destinée au dépôt et à la diffusion de documents scientifiques de niveau recherche, publiés ou non, émanant des établissements d'enseignement et de recherche français ou étrangers, des laboratoires publics ou privés.

Temperature Dependent Rate Constant for the Reaction of F-Atoms with HNO_3

YURI BEDJANIAN*

Institut de Combustion, Aérothermique, Réactivité et Environnement (ICARE), CNRS, 45071 Orléans Cedex 2, France

ABSTRACT: The kinetics of the reaction of F-atom with HNO_3, source of NO_3 radicals widely used in laboratory studies, has been investigated at nearly 2.7 mbar total pressure of helium over a wide temperature range, T = 220 – 700 K, using a low pressure discharge flow reactor combined with an electron impact ionization quadrupole mass spectrometer. The rate constant of the reaction F + $HNO_3 \rightarrow NO_3$ + HF (1) was determined using both relative rate method and absolute measurements under pseudo-first order conditions, monitoring the kinetics of F-atom consumption in excess of HNO_3, $k_1 = (6.1 \pm 0.4)\times10^{-12} \exp((155 \pm 18)/T)$ $cm^3 molecule^{-1} s^{-1}$ (where the uncertainties represent precision at the 2σ level, the estimated total uncertainty on k_1 being 15% at all temperatures). The reaction rate constant was found to be in excellent agreement with the only previous temperature dependent study. Experiments on detection of the reaction product, HF, have shown that NO_3 and HF forming channel of the title reaction is the dominant, if not unique, on the whole temperature range of the study.

Keywords: Fluorine atom, nitric acid, NO_3 radical, rate coefficient, temperature dependence.

*Correspondence to: Yuri Bedjanian: Tel.: +33 238255474, e-mail: yuri.bedjanian@cnrs-orleans.fr

INTRODUCTION

Nitrate radical (NO_3), which is formed in the atmosphere mainly in the reaction of NO_2 with ozone, is an important atmospheric oxidant, particularly in nighttime chemistry [1]. Understanding of the atmospheric photochemistry of NO_3 requires experimental kinetic and spectroscopic studies of the processes in which it is involved. Reaction

$$F + HNO_3 \rightarrow NO_3 + HF \qquad (1)$$

is a convenient source of nitrate radicals and is very often used for generation of NO_3 in laboratory studies. However, despite its frequent use and importance, the temperature dependence of the rate constant of reaction (1) was investigated in only one (for temperatures between 260 and 373 K [2]) from four available in the literature kinetic studies [2-5]. In this paper, we report the measurements of the rate constant of the reaction of fluorine atoms with nitric acid as a function of temperature in an extended temperature range, 220–700 K.

EXPERIMENTAL

Experiments were carried out in a discharge flow reactor using a modulated molecular beam electron ionization mass spectrometer as the detection method [6,7]. Two flow reactors were used. The first one, used at low temperatures (220 – 320 K), consisted of a Pyrex tube (45 cm length and 2.4 cm i.d.) with a jacket for the thermostated liquid circulation (ethanol). The walls of the reactor as well as of the movable injector of fluorine atoms were coated with halocarbon wax (HW) in order to minimize their heterogeneous loss. The second flow reactor used at high temperatures (T = 310 – 700 K), consisted of an electrically heated Quartz tube (45 cm length and 2.5 cm i.d.) with water-cooled attachments (Fig. 1) [8].

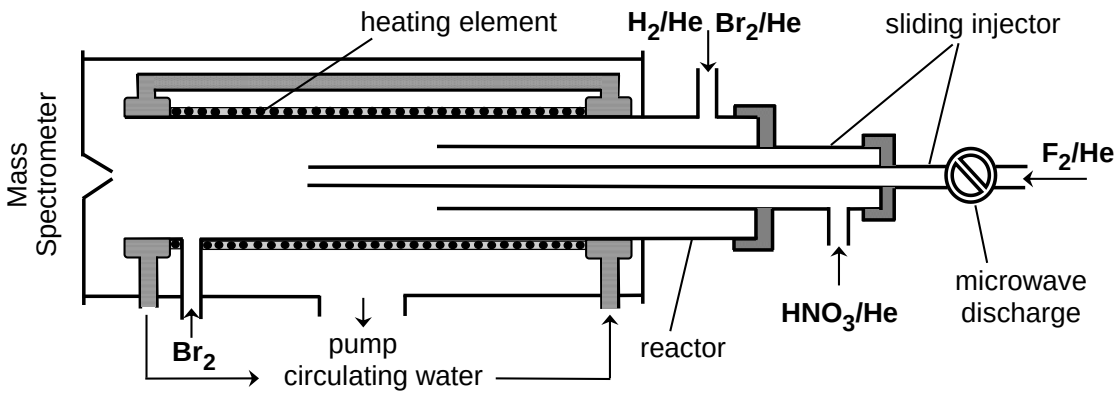

Figure 1 Diagram of the flow reactor.

Fluorine atoms were generated from the microwave discharge in F_2/He mixtures (Fig. 1). To reduce F atom reactions with glass surface inside the microwave cavity, a ceramic (Al_2O_3) tube was inserted into this part of the injector. Mass spectrometric monitoring of molecular fluorine showed that more than 90% of F_2 was dissociated in the microwave discharge. F-atoms were detected at m/z = 98/100 (FBr^+) after being scavenged with an excess of Br_2 (added in the end of the reactor 6 cm upstream of the sampling cone as shown in Fig. 1) through reaction (2):

$$F + Br_2 \rightarrow Br + FBr \qquad (2)$$

$k_2 = (1.28 \pm 0.20) \times 10^{-10}$ cm^3 molecule^{-1} s^{-1} (T = 299 – 940 K) [9].

This reaction was also used for the determination of the absolute concentrations of F-atoms through their chemical conversion to FBr in excess of Br_2: [F] = [FBr] = $\Delta[Br_2]$, i.e. concentration of F-atoms (FBr) was determined from the consumed fraction of $[Br_2]$.

The HNO_3 vapors were delivered to the reactor by flowing the bath gas (He) over thermostated (at nearly 0°C) HNO_3 (70% in water)/H_2SO_4 mixture (in an approximate 1:3 ratio) or from flask with a known HNO_3/He mixture and were detected by mass spectrometry at m/z = 63 and 46 (HNO_3^+ and NO_2^+). The H_2O impurity in the gaseous samples of HNO_3, directly detected at m/z =18 (H_2O^+), was always less than 1%. Absolute concentrations of HNO_3 as well of the other stable species (NO, NO_2, F_2, H_2 and Br_2) were calculated from their flow rates obtained from the measurements of the pressure drop of their mixtures in He stored in calibrated volume flasks. For absolute calibration of HNO_3 another method, linking HNO_3 and Br_2 concentrations, was also employed. It consisted in titration of the same concentration of F atoms with excess Br_2 ($[F]_0 = \Delta[Br_2]$) and HNO_3 ($[F]_0 = \Delta[HNO_3]$). This procedure allowed absolute calibration of HNO_3 signals using that of Br_2. The absolute concentrations of HNO_3 determined with two employed methods were consistent within 10%. All species were detected by mass spectrometry at their parent peaks: *m*/*z*= 63 (HNO_3^+), 46 (NO_2^+), 30 (NO^+), 160 (Br_2^+), 98/100 (BrF^+), 38 (F_2^+), 20 (HF^+), 18 (H_2O^+). The contribution of NO_2 at m/z = 30 (NO^+) due to fragmentation of NO_2 in the ion source of the mass spectrometer (operated at 25–30 eV energy) could be easily determined by simultaneous detection of the signals from NO_2 at *m*/*z*= 46 and 30.

RESULTS AND DISCUSSION

Rate Constant of reaction (1)

Absolute measurements. The rate constant of the title reaction was determined under pseudo-first order conditions monitoring F-atom decays in excess of HNO_3, $[F] = [F]_0 \times \exp(-k_1' \times t)$, where [F] and $[F]_0$ are the time-dependent and initial concentrations of F atoms, respectively, and $k_1' = k_1 \times [HNO_3] + k_w$ is the pseudo-first-order rate constant with k_w representing the loss of F atoms in the absence of nitric acid in the reactor. Initial concentration of fluorine atoms in these experiments was in the range $(2 - 5) \times 10^{11}$ molecule cm^{-3}; the concentrations of HNO_3 are shown in Table I. The flow velocity in the reactor was in the range (2210-3030) cm s^{-1}. The pseudo-first-order rate constants were determined from the exponential fit to F-atom consumption kinetics: an example is shown in Fig. 2.

Table I Reaction F + HNO_3: Summary of the Measurements of the Rate Constant

T (K)	number of kinetic runs	$[HNO_3]$ (10^{13}molecule cm^{-3})	k_1[a] ($10^{-11}cm^3molecule^{-1}s^{-1}$)	reactor surface[b]	method[c]
220	8	0.10-1.47	3.30	HW	AM
233	7	0.13-0.99	3.11	HW	AM
235	8	0.10-1.49	3.17	HW	AM
237	8	0.06-0.67	3.05	HW	AM
253	8	0.10-1.50	2.87	HW	AM
273	8	0.10-1.50	2.71	HW	AM
298	10	0.15-1.91	2.33	HW	AM
310	8	0.07-1.41	2.31	Q	AM
320	8	0.18-1.63	2.25	HW	AM
339	10	1.17-66.7	2.12	BA	RM
340	9	0.12-3.70	2.07	BA	AM
390	10	1.65-61.8	1.92	BA	RM
420	14	0.32-4.20	1.75	BA	AM
460	24	1.02-76.5	1.64	BA	RM
460	16	0.09-2.47	1.58	Q	AM
500	9	0.12-5.12	1.51	BA	AM
550	8	1.20-59.2	1.40	BA	RM
615	8	0.24-6.6	1.33	BA	AM
700	10	1.12-37.7	1.33	BA	RM

[a] Estimated uncertainty on k_1 is 15 and 20 % for absolute and relative rate measurements, respectively.
[b] HW: halocarbon wax; Q: quartz; BA: boric acid.
[c] AM: absolute measurements; RM: relative rate measurements.

The consumption of the excess reactant, HNO_3, was observed to be insignificant (within a few percent), although reaching up to 20 % in a few kinetic runs: in all cases the average

concentration of excess reactant along the reaction zone was used in the calculation of the reaction rate constant. Examples of the dependencies of the pseudo-first order rate constant, k_1', on concentration of excess reactant, HNO_3, at different temperatures are shown in Fig. 3.

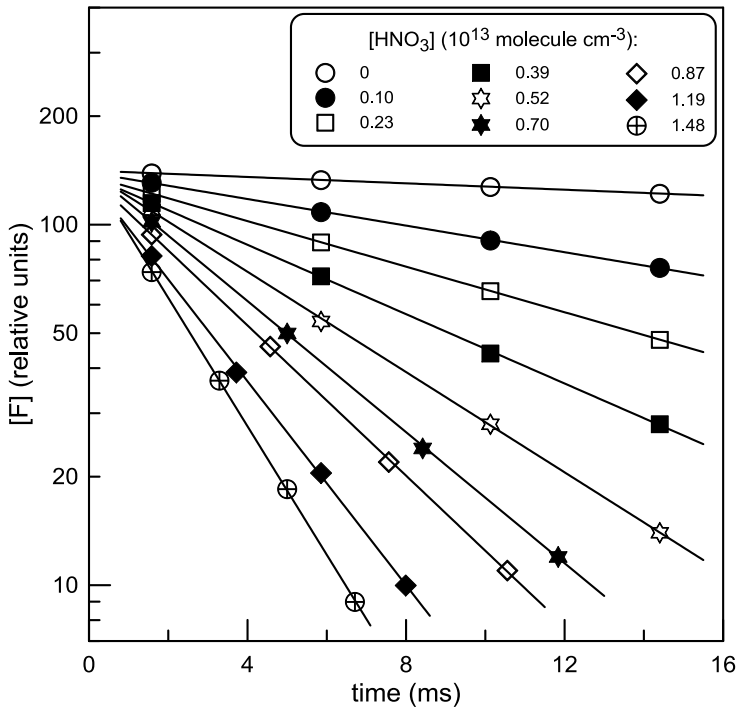

Figure 2 Examples of the pseudo-first-order decays of F-atom in reaction with HNO_3 observed at T=253 K. Uncertainty on the measurements of the relative concentrations of F-atom (≤ 5%) corresponds to the size of the symbols.

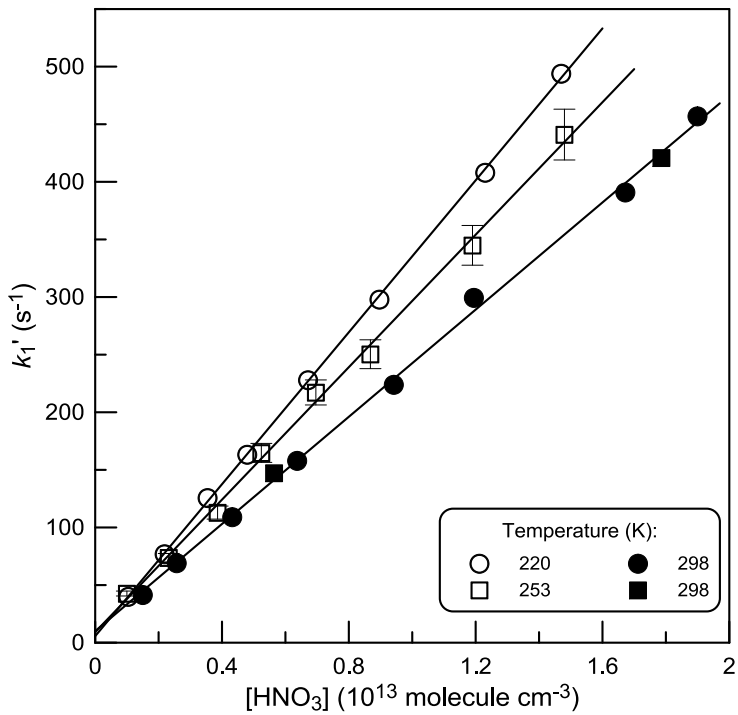

Figure 3 Pseudo-first-order rate constant (k_1') as a function of the concentration of HNO_3 measured at different temperatures in the reactor covered with halocarbon wax: filled squares represent the data observed at T = 298 K without addition of NO in the reactor (see text). Error bars represent typical uncertainties (≤ 5%) on the determination of k_1'.

All measured values of k_1' were corrected for axial and radial diffusion [10] of fluorine atoms. The diffusion coefficient of F-atom in He, $D_0 = 614\times(T/298)^{1.75}$ Torr cm^2 s^{-1} was estimated with Fuller's method [11]. Corrections were ≤ 10 %.

The possible impact of the secondary reaction

$$F + NO_3 \rightarrow FO + NO_2 \quad (3)$$

$k_3 = 3 \times 10^{-11}$ cm^3 molecule^{-1} s^{-1} (T = 298K) [4]

on the measurements of k_1 was insignificant due to relatively low initial concentrations of F atoms used. Even so, in the experiments on the measurements of k_1, NO ($(1 - 3) \times 10^{13}$ molecule cm^{-3}) was added into reactive system in order to quantitatively suppress the possible secondary consumption of F atoms. In fact, NO inhibits the secondary chemistry through scavenging of NO_3 radicals,

$$NO + NO_3 \rightarrow NO_2 + NO_2 \quad (4)$$

$k_4 = 1.5 \times 10^{-11}\exp(170/T)$ cm^3 molecule^{-1} s^{-1} (T = 209-703 K) [12],

and, on the other hand, does not contribute to F atom consumption under experimental conditions of the study,

$$F + NO\ (+M) \rightarrow FNO\ (+ M) \quad (5),$$

k_5 being $< 2 \times 10^{-14}$ cm^3 molecule^{-1} s^{-1} at P = 2.7 mbar and T = 220-700 K [12].

The intercepts in the examples shown in Fig. 3 (as well as in all the experiments carried out at low temperatures in the reactor coated with halocarbon wax), k_w, were in the range (3 - 10) s^{-1}, in good agreement with the rate of F-atom decay measured in the absence of HNO_3 in the reactor. However; in experiments with the uncoated quartz reactor at higher temperatures, the rate of F-atom consumption rapidly increased upon addition of even very low concentrations of HNO_3 ($< 7\times10^{11}$ molecule cm^{-3} in Fig. 4). As one can see in Fig. 4, the intercept of the linear fit to the experimental data (≈ 70 s^{-1}) is much higher than the value of k_w (≈ 10 s^{-1}) measured in the absence of HNO_3 in the reactor. The observed effect did not depend on the manner of HNO_3 delivery to the reactor (from flask with a known HNO_3/He mixture or flowing helium over a liquid HNO_3) and did not seem to be related to the secondary chemistry, as shown in experiments with and without addition of NO in the reactor (Fig. 4). Becker et al. [5] reported a similar effect at T = 298 K in experiments with uncoated quartz reactor and not in the reactor coated with halocarbon wax. The observation was

attributed to the heterogeneous reaction between F atoms and HNO_3, predominant at low concentrations of HNO_3 [5].

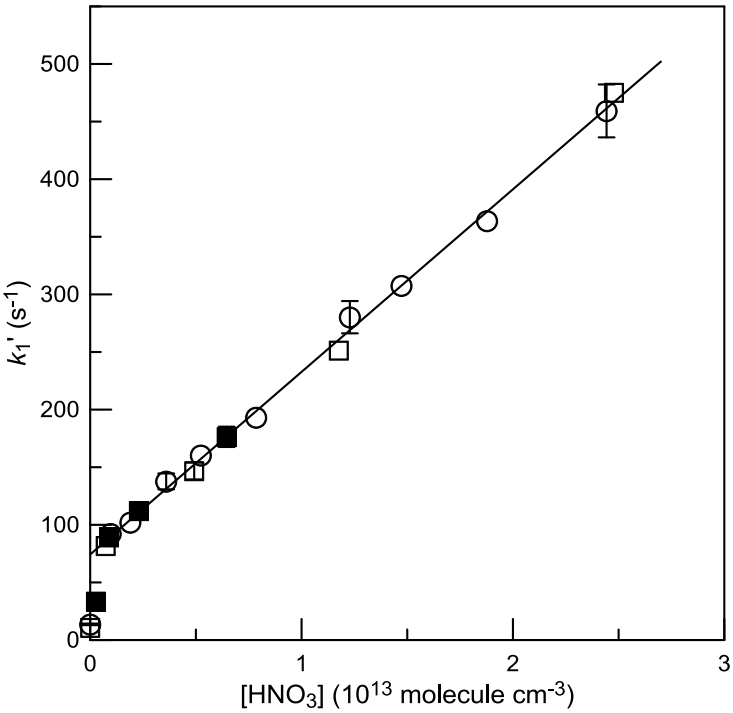

Figure 4 Pseudo-first-order rate constant (k_1') as a function of the concentration of HNO_3 measured at T = 460 K in an uncoated quartz reactor: circles and squares represent the data observed with and without addition of NO in the reactor, respectively; filled and open symbols represent experiments with HNO_3 introduced into the reactor from flask with a known HNO_3/He mixture and flowing helium over a liquid HNO_3, respectively.

Seeking to reduce the heterogeneous loss of F-atoms in the presence of HNO_3 in the reactor, we have coated the reactor with boric acid. However, this approach did not alleviate the observed effect: at all temperatures of the measurements the intercept (40 -100 s^{-1}) of the linear fit to the experimental values of k_1' as a function of [HNO_3] was always much higher than F-atom loss observed in the absence of nitric acid in the reactor (10-20 s^{-1}). This heterogeneous effect was not strongly correlated with temperature and could be reduced upon prolonged (~ 1 hour) exposure of the reactor to the reaction mixture. Examples of the data observed in boric acid coated reactor are shown in Fig. 5. Ultimately, the reaction rate constant was determined from the slope of the linear fit to the experimental data observed at relatively high concentrations of HNO_3 (straight lines in Figs. 4 and 5), i.e. under assumption that heterogeneous contribution to the loss of F-atoms is independent of HNO_3 concentration in the gas phase under these conditions and considering that the intercept is much lower than the measured maximum values of k_1'. All the results of the absolute measurements of k_1 are shown in Table I. The combined uncertainty on k_1 was estimated to be ≈15% by adding in

quadrature statistical error (≤ 5%) and those on the measurements of the flows (5%), pressure (3%), temperature (1%) and absolute concentration of HNO_3 (≤ 10%).

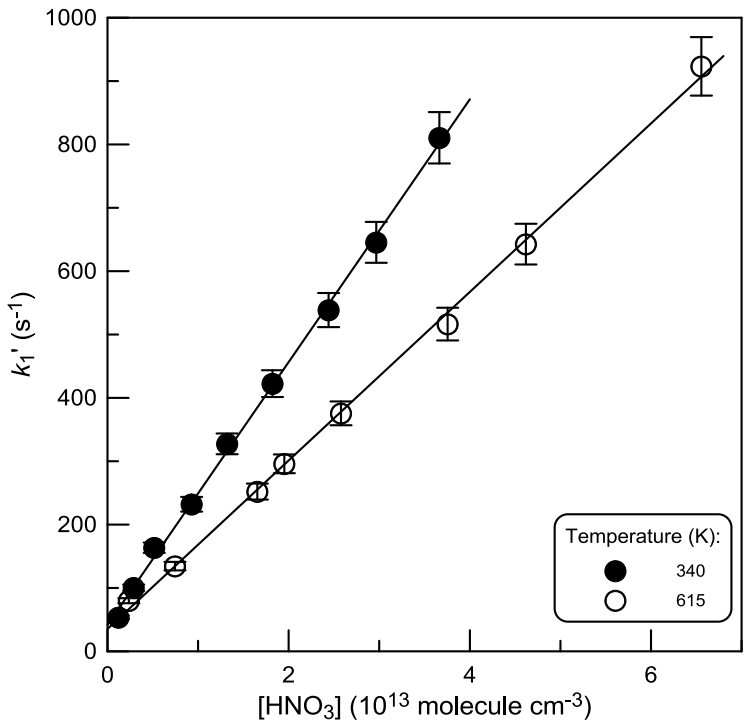

Figure 5 Pseudo-first-order rate constant (k_1') as a function of the concentration of HNO_3 measured in the reactor coated with boric acid. Error bars represent typical uncertainties (≤ 5%) on the determination of k_1'.

Relative rate measurements. Given the possible heterogeneous complications in the absolute measurements of the reaction rate constant at elevated temperatures (in quartz and boric acid coated reactors), we have carried out relative rate measurements with reaction of F atoms with Br_2 as reference:

$$F + Br_2 \rightarrow FBr + Br \qquad (2)$$

In these experiments, fast titration of the initial concentration of F atoms, $[F]_0$, by a mixture of excess HNO_3 and Br_2 was performed, and the yield of FBr was measured as a function of the $[HNO_3]/[Br_2]$ ratio. The concentration of FBr formed is defined by the fraction of $[F]_0$ reacting with Br_2 in reaction 2:

$$[FBr] = \frac{k_2[Br_2]}{k_2[Br_2]+k_1[HNO_3]+k_w} \times [F]_0$$

Rearrangement of this expression leads to:

$$\frac{[F]_0}{[FBr]} - 1 = \frac{k_1[HNO_3]}{k_2[Br_2]} + \frac{k_w}{k_2[Br_2]} \qquad (I)$$

Experiments were carried out at constant concentration of Br_2 (to keep the contribution of the second term in equation (I) constant) and k_1/k_2 could be obtained by plotting ($[F]_0/[FBr]$ - 1)

as a function of the $[HNO_3]/[Br_2]$ ratio. This method did not need the measurements of the absolute concentrations FBr and F-atoms because the initial concentration of F-atoms, $[F]_0$, could be expressed as FBr signal in the absence of HNO_3 in the reactor, when F is titrated with an excess of Br_2. Thus, in the experiments, only the FBr signal was detected: first, in HNO_3-free system, corresponding to $[F]_0$, and then in the Br_2 and HNO_3-containing system, corresponding to the fraction of $[F]_0$ reacted with Br_2. Reaction time was around 0.01 s, initial concentration of F atoms was varied in the range $(1.0\text{-}2.5)\times10^{12}$ molecule cm^{-3}, concentration of Br_2 was (3-4))$\times10^{13}$ molecule cm^{-3} , those of HNO_3 are shown in Table I. All the measurements were conducted in the presence of NO in the reactor in order to remove NO_3, product of the reaction (1), and to reduce (although insignificant under operating conditions) the impact of the secondary reaction F + NO_3. Examples of the observed experimental data are shown in Fig. 6. The variation of the initial concentration of F-atoms (T = 339 K) and that of NO (T = 460 K) had no impact on the results of the measurements. According to equation (I), the slopes of the linear dependences in Fig. 6 provide the values of k_1/k_2 at respective temperatures. Final values of k_1, calculated with independent of temperature k_2 = $(1.28 \pm 0.20)\times10^{-10}$ $cm^3 molecule^{-1} s^{-1}$ (T = 299 - 940K) [9] are presented in Table I.

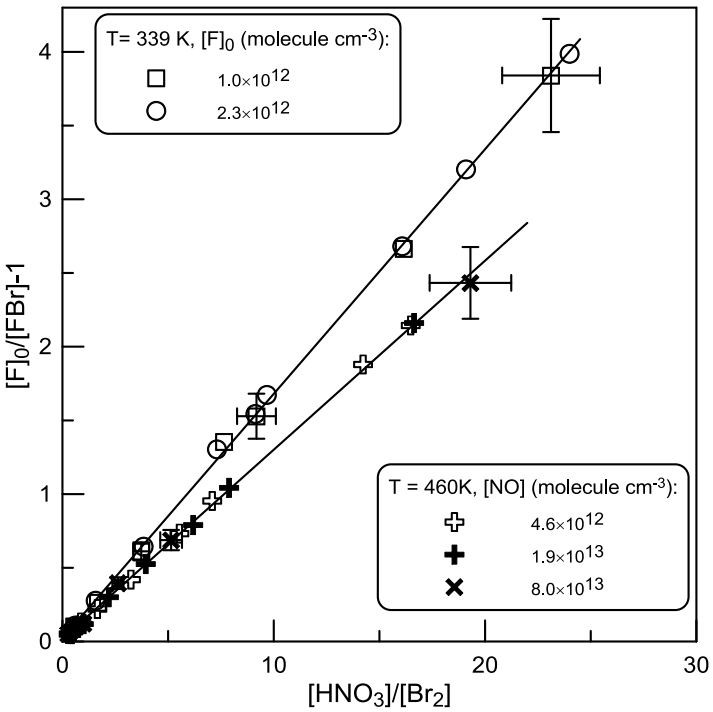

Figure 6 FBr yield from F-atom titration with HNO_3 + Br_2 mixtures at T = 339 and 460 K. The horizontal and vertical error bars represent estimated (of nearly 10 %) uncertainties on the respective values.

Reaction products

Although the NO_3-forming route of the reaction (1) is generally considered as the main one, two other exothermic channels are available for the reaction:

$$F + HNO_3 \rightarrow NO_3 + HF \qquad \Delta_r H° = -143.7 \text{ kJ mol}^{-1} \qquad (1a)$$

$$\rightarrow OH + FNO_2 \qquad \Delta_r H° = -22.5 \text{ kJ mol}^{-1} \qquad (1b)$$

$$\rightarrow HO_2 + FNO \qquad \Delta_r H° = -20.4 \text{ kJ mol}^{-1} \qquad (1c)$$

The thermochemical data used for the calculations of $\Delta_r H°$ are from ref. [12]. In order to obtain experimental evidence of the dominance of the reaction channel (1a) both at low and high temperatures of the study, we have carried out additional experiments on the detection of the product of reaction (1), HF. Experiments consisted in a successive titration of the initial concentration of F-atom with an excess H_2 and HNO_3 accompanied with a direct detection of the reaction product, HF. This allowed to measure the yield of HF in the reaction of F-atom with HNO_3 relatively to that in the reaction of F with H_2, where the yield of HF is 100%. The advantage of this approach is that it does not require the measurements of the absolute concentrations of either F-atoms or HF. Experiments have been carried out at two temperatures: 235 and 615 K. Reaction time was nearly 0.02 ms, $[HNO_3] \approx 3\times10^{13}$ and 10^{14}, $[H_2] \approx 6\times10^{13}$ and 2×10^{13}, $[F]_0 = (0.25\text{-}3.6) \times10^{12}$ and $(0.15\text{-}3.1) \times10^{12}$ molecule cm^{-3}at T = 235 and 615 K, respectively. The observed data are shown in Fig. 7.

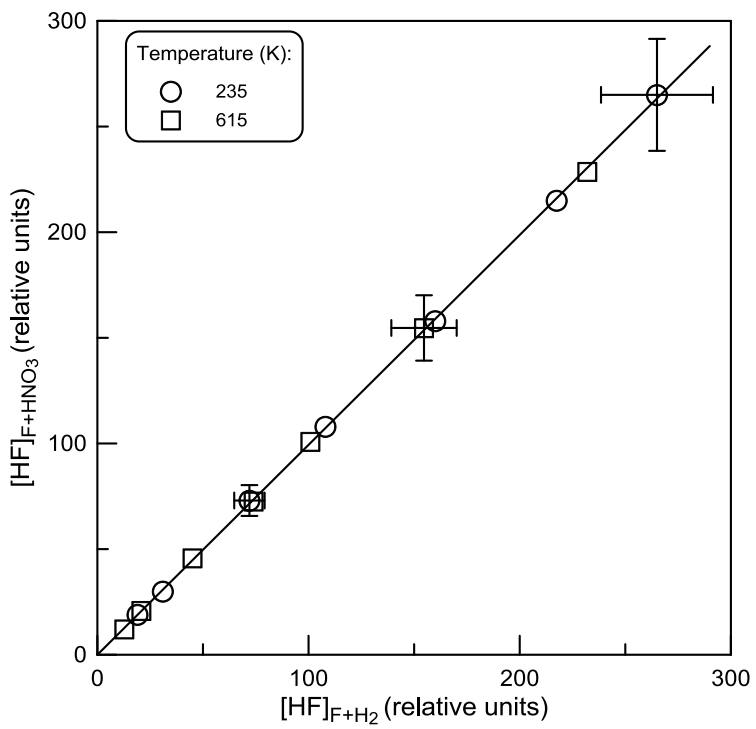

Figure 7 Concentration of HF formed in reaction of F-atom with HNO_3 as a function of the concentration of HF formed in F-atom reaction with H_2 upon consumption of the same concentration of F-atoms. Error bars correspond to the upper limit (of 10%) of the uncertainty on the determination of the relative concentrations.

The linear through origin fit to all the data observed at two temperatures (straight line in Fig. 7) provides independent of temperature branching ratio for the HF forming channel of reaction (1): 0.993 ± 0.005 (2σ), indicating that that NO_3+HF pathway of the reaction (1) is the dominant one in the temperature range of the present study.

Comparison with previous data

Figure 8 summarizes the results of previous and current measurements of the rate constant of reaction (1). Mellouki et al. [3] have measured the reaction rate constant at T = 298 K in a fast-flow reactor combined with electron spin resonance (ESR) spectroscopy: k_1 = (2.7 ± 0.5)×10^{-11} $cm^3molecule^{-1}s^{-1}$. Rahman et al. [4], using flow reactor combined with mass spectrometry as a detection method have reported k_1 = (2.1 ± 1.0)×10^{-11} $cm^3molecule^{-1}s^{-1}$ at T = 298 K which was derived from kinetics of the products of reaction (1), HF and NO_3, and from the kinetics of HNO_3 consumption in excess of F atoms. Afterwards the rate constant has been re-determined in the same group, k_1 = (2.2 ± 0.2)×10^{-11} $cm^3molecule^{-1}s^{-1}$ at T = 298 K, employing fast flow system and following NO_3 formation and F-atom decays by mass spectrometry and ESR method, respectively [5]. Results of these room temperature measurements of k_1 are in agreement with the present data in the range of the reported experimental uncertainties. In the only temperature dependent study of reaction (1), Wine et al. [2] used a time-resolved long-path laser absorption technique to monitor the kinetics of reaction product, NO_3 radical, upon pulsed laser photolysis of F_2/HNO_3/He mixture in the temperature range 260-373 K. The authors represented k_1 by the Arrhenius expression k_1 = (6.0 ± 2.6)×10^{-12} exp((400 ± 120)/T) between 260 and 320 K and with independent of temperature value of k_1 = (2.0 ± 0.3)×10^{-11} $cm^3molecule^{-1}s^{-1}$ in the temperature range 335-373 K. As one can see in Fig. 8, the present measurements do not confirm the independence of k_1 of temperature at T > 335 K, showing negative temperature dependence of k_1 in the whole temperature range of this study, 220-700 K. At the same time, the absolute values of k_1 measured by Wine et al. [2] are in excellent agreement with the present data which can be represented by the following Arrhenius expression:

$$k_1 = (8.2 \pm 0.4)\times10^{-12} \exp((315 \pm 15)/T)\ cm^3molecule^{-1}s^{-1}$$

between 220 and 700 K and with 2σ uncertainties representing the precision of the fit.

The observed negative temperature dependence of the reaction rate constant may be considered as an indication of a complex reaction mechanism that includes formation of an intermediate energized F•HNO_3 adduct followed either by its dissociation back to reactants or to reaction products. Similar mechanism was proposed for analogous reaction OH + HNO_3 → NO_3 + H_2O (e.g. [13]). The rate constant of the reaction OH + HNO_3 was found to be pressure dependent below room temperature (e.g. [14]). In this context, we have checked for the possible pressure dependence of the rate constant of the reaction F+HNO_3 in the lower temperature range covered in the present study. The values of k_1 at T = 233, 235 and 237 K presented in Table I and Fig. 8 were measured at total pressure of 0.67, 2.7 and 6.7 mbar, respectively. As one can note, k_1 was found to be pressure independent in the range of the experimental uncertainty (at least, at low temperatures of the present study), although this does not exclude a possible pressure dependence of k_1 at higher pressures.

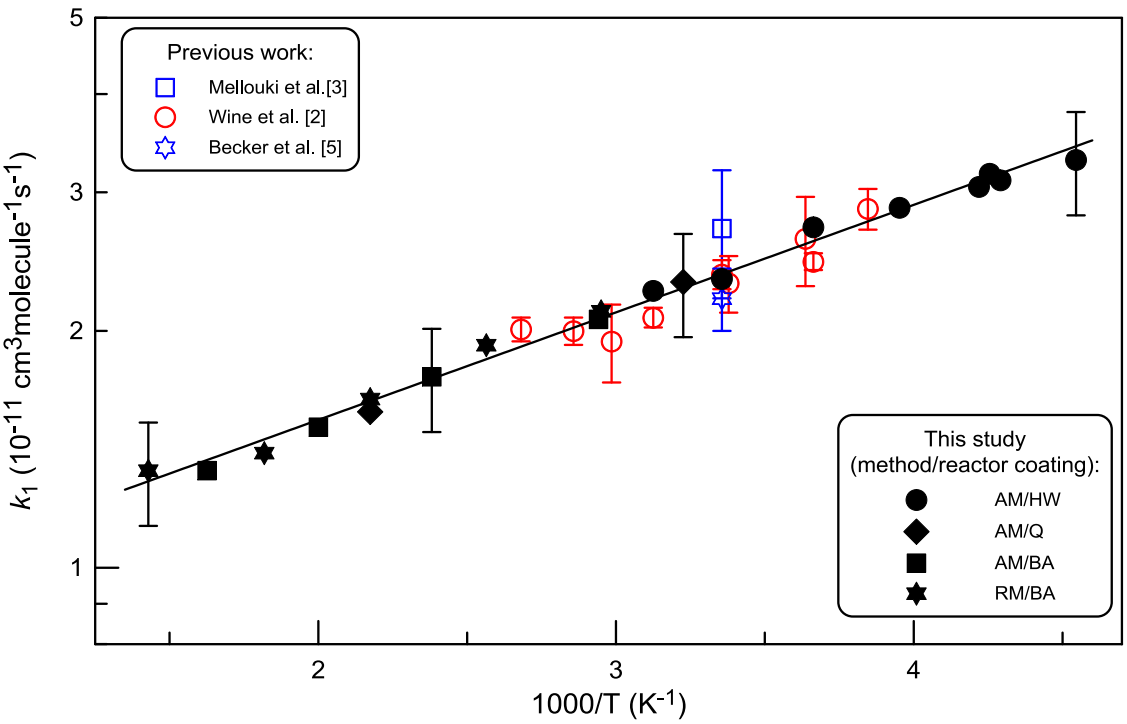

Figure 8 Summary of the measurements of the rate constant of reaction (1). AM: absolute measurements; RM: relative measurements; HW: halocarbon wax; Q: quartz; BA: boric acid. Partially shown error bars on the present data correspond to estimated 15 % uncertainty on the measurements of k_1. Uncertainties on k_1 reported in previous studies correspond to 2σ [2,5] and total estimated uncertainty [3].

CONCLUSION

In this work, using a discharge-flow reactor combined with mass spectrometry, we have measured the rate constant of the reaction of fluorine atoms with nitric acid as a function of temperature in an extended temperature range, 220–700 K. The

temperature dependence of the rate constant of this reaction, very often used as a source of NO_3 radical (important intermediate in nighttime atmospheric chemistry) in laboratory, was found to be in good agreement with the only other temperature dependent study at T = 260-373 K and was extended to lower (220K) and higher (700K) temperatures. Experiments on detection of the reaction product, HF, have shown that the NO_3 and HF forming channel of the title reaction is dominant, if not quantitative one in the whole temperature range of the study. The negative temperature dependence of the rate constant seems to indicate a complex reaction mechanism, probably, involving formation of long lived intermediate complex followed by its rearrangement and dissociation to products.

Financial support from CNRS is gratefully acknowledged.

BIBLIOGRAPHY

1. Wayne, R. P.; Barnes, I.; Biggs, P.; Burrows, J. P.; Canosa-Mas, C. E.; Hjorth, J.; Le Bras, G.; Moortgat, G. K.; Perner, D.; Poulet, G.; Restelli, G.; Sidebottom, H. The nitrate radical: Physics, chemistry, and the atmosphere. Atmos. Environ. 1991, 25A, 1-203.
2. Wine, P. H.; Wells, J. R.; Nicovich, J. M. Kinetics of the reactions of atomic fluorine(^{2}P) and atomic chlorine(^{2}P) with nitric acid. J. Phys. Chem. 1988, 92, 2223-2228.
3. Mellouki, A.; Le Bras, G.; Poulet, G. Discharge flow kinetic study of nitrate radical reactions with free radicals: the reaction of nitrate radical with chlorine atom. J. Phys. Chem. 1987, 91, 5760-5764.
4. Rahman, M. M.; Becker, E.; Benter, T.; Schindler, R. N. A Gasphase Kinetic Investigation of the System F + HNO_3 and the Determination of Absolute Rate Constants for the Reaction of the NO_3 Radical with CH_3SH, 2-Methylpropene, 1,3-Butadiene and 2,3-Dimethyl-2-Butene. Ber. Bunsenges. Phys. Chem. 1988, 92, 91-100.
5. Becker, E.; Benter, T.; Kampf, R.; Schindler, R. N.; Wille, U. A Redetermination of the Rate Constant of the Reaction F + HNO_3 → HF + NO_3. Ber. Bunsenges. Phys. Chem. 1991, 95, 1168-1173.
6. Bedjanian, Y. Reaction F + C_2H_4: Rate Constant and Yields of the Reaction Products as a Function of Temperature over 298–950 K. J. Phys. Chem. A 2018, 122, 3156-3162.
7. Bedjanian, Y.; Lelièvre, S.; Le Bras, G. Kinetic and mechanistic study of the F atom reaction with nitrous acid. J. Photochem. Photobio. A 2004, 168, 103-108.
8. Morin, J.; Romanias, M. N.; Bedjanian, Y. Experimental Study of the Reactions of OH Radicals with Propane, n-Pentane, and n-Heptane over a Wide Temperature Range. Int. J. Chem. Kinet. 2015, 47, 629-637.
9. Bedjanian, Y. Kinetics and Products of the Reactions of Fluorine Atoms with ClNO and Br_2 from 295 to 950 K. J. Phys. Chem. A 2017, 121, 8341-8347.
10. Kaufman, F. Kinetics of Elementary Radical Reactions in the Gas Phase. J. Phys. Chem. 1984, 88, 4909-4917.

11. Tang, M. J.; Cox, R. A.; Kalberer, M. Compilation and evaluation of gas phase diffusion coefficients of reactive trace gases in the atmosphere: volume 1. Inorganic compounds. Atmos. Chem. Phys. 2014, 14, 9233-9247.
12. Burkholder, J. B.; Sander, S. P.; Abbatt, J.; Barker, J. R.; Huie, R. E.; Kolb, C. E.; Kurylo, M. J.; Orkin, V. L.; Wilmouth, D. M.; Wine, P. H. Chemical Kinetics and Photochemical Data for Use in Atmospheric Studies, Evaluation No. 18, JPL Publication 15-10, Jet Propulsion Laboratory, Pasadena, 2015 http://jpldataeval.jpl.nasa.gov, accessed March 2019.
13. Brown, S. S.; Burkholder, J. B.; Talukdar, R. K.; Ravishankara, A. R. Reaction of hydroxyl radical with nitric acid: insignts into its mechanism. J. Phys. Chem. A 2001, 105, 1605-1614.
14. Brown, S. S.; Talukdar, R. K.; Ravishankara, A. R. Reconsideration of the Rate Constant for the Reaction of Hydroxyl Radicals with Nitric Acid. J. Phys. Chem. A 1999, 103, 3031-3037.

TABLES

Table I Reaction F + HNO_3: Summary of the Measurements of the Rate Constant

T (K)	number of kinetic runs	[HNO_3] (10^{13}molecule cm^{-3})	k_1[a] (10^{-11}cm^{3}molecule^{-1}s^{-1})	reactor surface[b]	method[c]
220	8	0.10-1.47	3.30	HW	AM
233	7	0.13-0.99	3.11	HW	AM
235	8	0.10-1.49	3.17	HW	AM
237	8	0.06-0.67	3.05	HW	AM
253	8	0.10-1.50	2.87	HW	AM
273	8	0.10-1.50	2.71	HW	AM
298	10	0.15-1.91	2.33	HW	AM
310	8	0.07-1.41	2.31	Q	AM
320	8	0.18-1.63	2.25	HW	AM
339	10	1.17-66.7	2.12	BA	RM
340	9	0.12-3.70	2.07	BA	AM
390	10	1.65-61.8	1.92	BA	RM
420	14	0.32-4.20	1.75	BA	AM
460	24	1.02-76.5	1.64	BA	RM
460	16	0.09-2.47	1.58	Q	AM
500	9	0.12-5.12	1.51	BA	AM
550	8	1.20-59.2	1.40	BA	RM
615	8	0.24-6.6	1.33	BA	AM
700	10	1.12-37.7	1.33	BA	RM

[a] Estimated uncertainty on k_1 is 15 and 20 % for absolute and relative rate measurements, respectively.
[b] HW: halocarbon wax; Q: quartz; BA: boric acid.
[c] AM: absolute measurements; RM: relative rate measurements.

FIGURE LEGENDS

Figure 1 Diagram of the flow reactor.

Figure 2 Examples of the pseudo-first-order decays of F-atom in reaction with HNO_3 observed at T=253 K. Uncertainty on the measurements of the relative concentrations of F-atom (≤ 5%) corresponds to the size of the symbols.

Figure 3 Pseudo-first-order rate constant (k_1') as a function of the concentration of HNO_3 measured at different temperatures in the reactor covered with halocarbon wax: filled squares represent the data observed at T = 298 K without addition of NO in the reactor (see text). Error bars represent typical uncertainties (≤ 5%) on the determination of k_1'.

Figure 4 Pseudo-first-order rate constant (k_1') as a function of the concentration of HNO_3 measured at T = 460 K in an uncoated quartz reactor: circles and squares represent the data observed with and without addition of NO in the reactor, respectively; filled and open symbols represent experiments with HNO_3 introduced into the reactor from flask with a known HNO_3/He mixture and flowing helium over a liquid HNO_3, respectively.

Figure 5 Pseudo-first-order rate constant (k_1') as a function of the concentration of HNO_3 measured in the reactor coated with boric acid. Error bars represent typical uncertainties (≤ 5%) on the determination of k_1'.

Figure 6 FBr yield from F-atom titration with HNO_3 + Br_2 mixtures at T = 339 and 460 K. The horizontal and vertical error bars represent estimated (of nearly 10 %) uncertainties on the respective values.

Figure 7 Concentration of HF formed in reaction of F-atom with HNO_3 as a function of the concentration of HF formed in F-atom reaction with H_2 upon consumption of the same concentration of F-atoms. Error bars correspond to the upper limit (of 10%) of the uncertainty on the determination of the relative concentrations.

Figure 8 Summary of the measurements of the rate constant of reaction (1). AM: absolute measurements; RM: relative measurements; HW: halocarbon wax; Q: quartz; BA: boric acid. Partially shown error bars on the present data correspond to estimated 15 % uncertainty on the measurements of k_1. Uncertainties on k_1 reported in previous studies correspond to 2σ [2,5] and total estimated uncertainty [3].